LETTER | AUGUST 05 2022

Resonant three-wave interactions with linear source/sink terms: Exploring the parameter space FREE

Y. Yakusevich ; S. I. Krasheninnikov

Physics of Plasmas 29, 080701 (2022)
https://doi.org/10.1063/5.0098271
CHORUS

Physics of Plasmas LETTER scitation.org/journal/php

Resonant three-wave interactions with linear source/sink terms: Exploring the parameter space

Cite as: Phys. Plasmas **29**, 080701 (2022); doi: 10.1063/5.0098271
Submitted: 6 May 2022 · Accepted: 8 July 2022 ·
Published Online: 5 August 2022

Y. Yakusevich[a] and S. I. Krasheninnikov

AFFILIATIONS

University of California San Diego, La Jolla, California 92038, USA

[a]Author to whom correspondence should be addressed: yyakusevich@ucsd.edu

ABSTRACT

It is shown that the resonance three wave interactions in the presence of linear source/sink terms exhibit a wide variety of time-evolution dynamics, such as exponential growth, limit cycles, and strange attractors. The particular features of the dynamics are determined primarily by the values of linear growth rates, forming a 2D parameter space. An exploration of this parameter space is the main focus of this present work.

The study of nonlinear wave interactions has applications in a diverse range of scientific disciplines, including liquids,[1] atmospheric waves,[2,3] waves in solids,[4] chemical reactions,[5] biological systems,[6] Bose–Einstein condensates,[7] and especially plasmas.[8–14] These interactions become particularly strong in the case of the resonant interactions, i.e., for the case of three-wave interactions, the wavevectors and frequencies obey the following relations:

$$\vec{k}_1 = \vec{k}_2 + \vec{k}_3, \quad \omega_{\vec{k}_1} = \omega_{\vec{k}_2} + \omega_{\vec{k}_3}.$$

Most of the studies on these wave–wave interactions assume that the individual waves participating in these interactions are neutrally stable. However, in Refs. 15–18, it was shown that the dynamics of the wave interactions could be drastically changed for the case where linear source/sink terms, characterized by positive and negative growth rates, are added to the equations governing the wave amplitudes. In particular, in Ref. 17, it was demonstrated that for the case of the ensemble of many interacting waves, an addition of the sink/source terms results in the bifurcation of the wave energy.[17] Whereas in Ref. 18, it was shown that for the case of three-wave interactions, the dynamics of the wave amplitudes have the features of a strange attractor (see Refs. 19–23). In plasma physics, this resonance interaction is typical for quadratic nonlinearities of the governing equations and is usually called the decay interaction.

In the latter case, the time evolution of the normalized wave amplitudes, $a_i(t)$, $i = 1, 2, 3$, is described by the following equations (e.g., see Ref. 18 and the references therein):

$$\begin{cases} \dfrac{da_1}{dt} = \gamma_1 a_1 + a_2 a_3, \\ \dfrac{da_2}{dt} = \gamma_2 a_2 - a_1 a_3, \\ \dfrac{da_3}{dt} = \gamma_3 a_3 - a_1 a_2, \end{cases} \tag{1}$$

where we assume that a_i is real and γ_i is the linear growth rates of the modes. Apart of a trivial case $a_i = 0$, the system (1) has the following stationary solutions $a_i \equiv \bar{a}_i$:

$$\bar{a}_1^2 = \gamma_2\gamma_3, \quad \bar{a}_2^2 = -\gamma_1\gamma_3, \quad \bar{a}_3^2 = -\gamma_1\gamma_2, \tag{2}$$

which also satisfy the relation $\bar{a}_1\bar{a}_2\bar{a}_3 = -\gamma_1\gamma_2\gamma_3 \equiv \gamma_g^3$. The analysis of the Manley-Rowe quadratic forms and stability of the stationary solutions (2) suggests that the most interesting dynamic of the wave amplitudes corresponds to the case where $\gamma_1 > 0$, $\gamma_2, \gamma_3 < 0$, and $\gamma_a = (\gamma_1 + \gamma_2 + \gamma_3)/3 < 0$.[18] In this case, the variables in Eq. (1) can be re-normalized as follows: $a_i\gamma_i \to a_i$ and $t\gamma_1 \to t$, and new effective growth rates $\hat{\gamma}_1 \equiv \gamma_1/\gamma_1 = 1$, $\hat{\gamma}_2 \equiv \gamma_2/\gamma_1$, and $\hat{\gamma}_3 \equiv \gamma_3/\gamma_1$ can be introduced. As a result, the solution of Eq. (1) depends only on initial conditions and the magnitudes of $\hat{\gamma}_2$ and $\hat{\gamma}_3$. In what follows, we will use Eq. (1), assuming that $\gamma_1 = 1$ and remove the "hats" from $\hat{\gamma}_2$ and $\hat{\gamma}_3$.

The main goal of this work is to explore numerically an impact of initial conditions and the magnitudes of γ_2 and γ_3 on the dynamics of the solutions of Eq. (1). All simulations were performed with the MATLAB built-in "ode89" solver. We found that the initial conditions

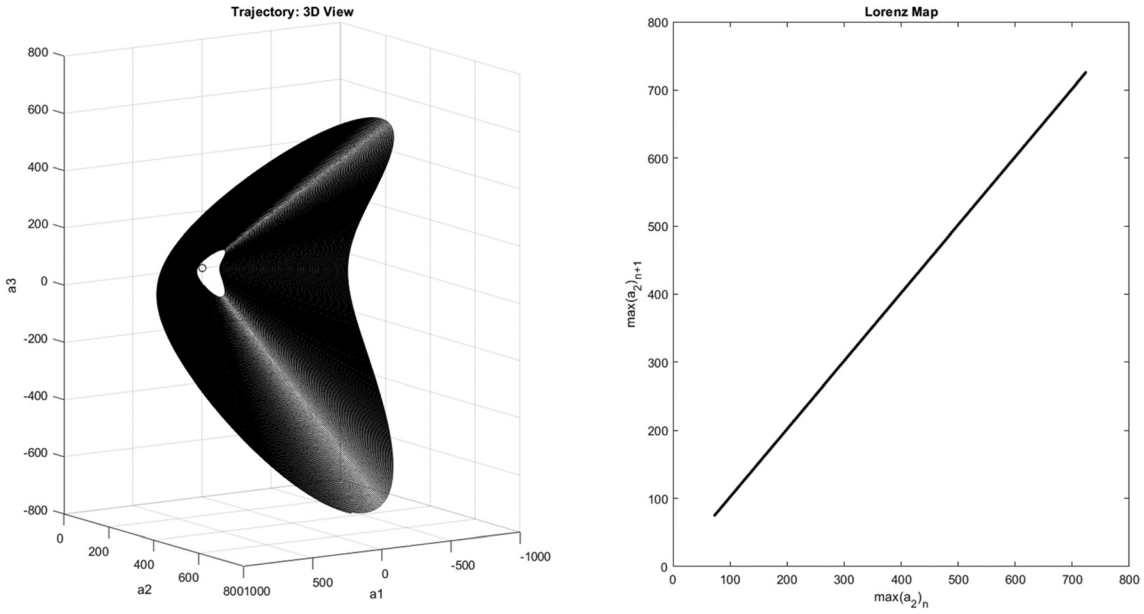

FIG. 1. Unbounded oscillating trajectory $a_i(t)$ and the Lorenz map (right) found for $\gamma_2 = 0.5$ and $\gamma_3 = 0.75$.

virtually do not alter the character of the trajectory $a_i(t)$ at large time (see examples below). Therefore, for the results shown in Figs. 1–6, we use the initial conditions $a_i(t = 0) = (1, 1, 0)$ and integrate Eq. (1) on the time interval (0, 5000) with the maximum time step capped at 0.1.

The results of our simulations reveal that depending on the magnitudes of γ_2 and γ_3, the solutions of Eq. (1) are characterized by (a) unbounded oscillating trajectories $a_i(t)$ and (b) the trajectories which at large time converge into a finite volume of the variables a_i.

The former ones could be characterized as:

(i) Exponential growth, see Fig. 1.

(ii) Asymptotic growth and explosive instability, which occur under certain conditions.[24]

The latter ones could be characterized as:

(i) Limit cycles with varying degrees of ergodicity, see Figs. 2–6.
(ii) Strange attractors, see Fig. 7.
(iii) "Multi-lobe" strange attractors, see Fig. 8.

To elucidate the difference between various types of trajectories, in Figs. 1–8, we also show the "Lorenz maps" corresponding to each type of trajectory. We define the "Lorenz map" as the function relating

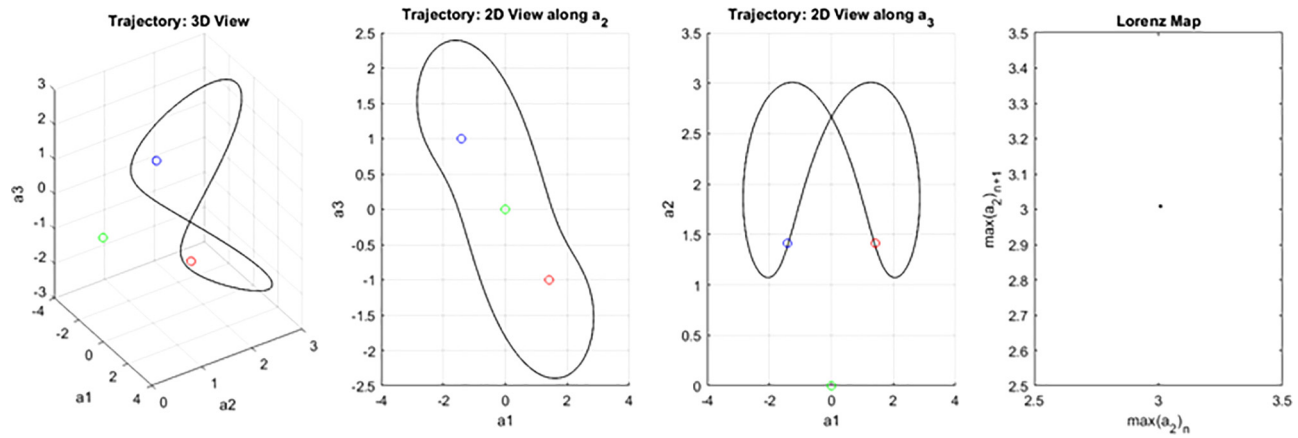

FIG. 2. The trajectory $a_i(t)$ converging to a pure limit cycle and the Lorenz map (right) found for $\gamma_2 = -1$ and $\gamma_3 = -2$. Note the extremely small radius of the Lorenz map.

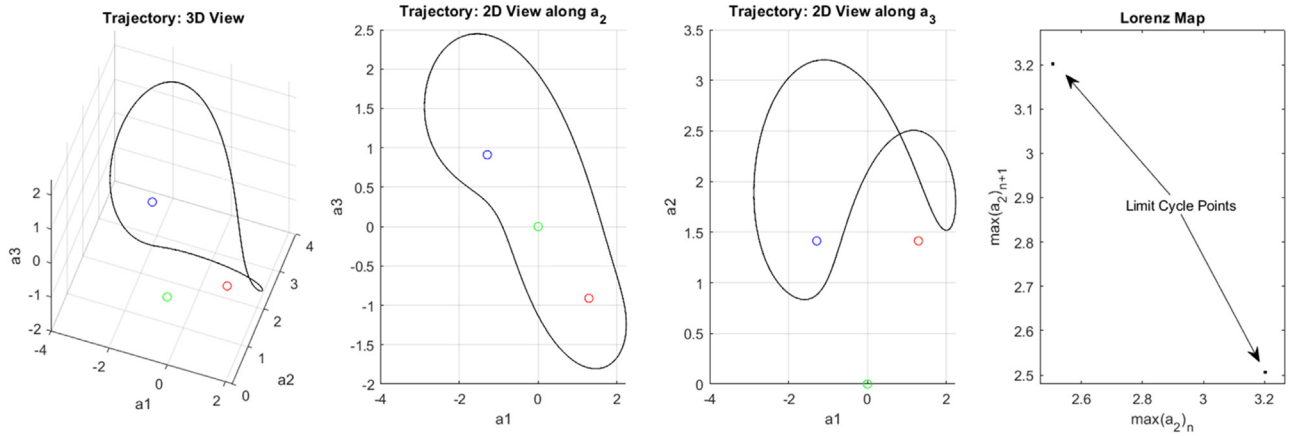

FIG. 3. The trajectory $a_i(t)$ converging to an uneven limit cycle and the Lorenz map (right) found for $\gamma_2 = -0.83$ and $\gamma_3 = -2$.

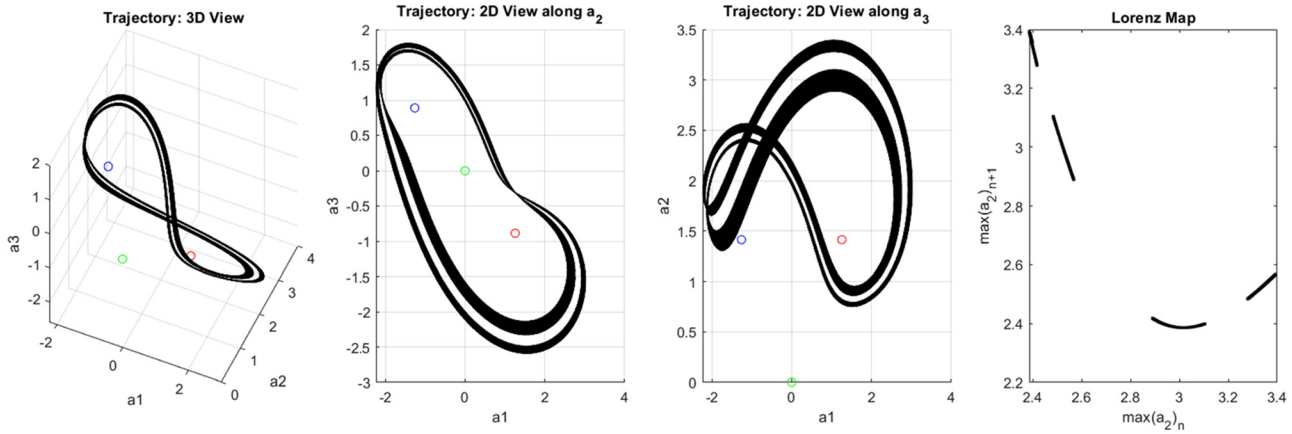

FIG. 4. The trajectory $a_i(t)$ converging to an ergodic limit cycle and the Lorenz map (right) found for $\gamma_2 = -0.79$ and $\gamma_3 = -2$.

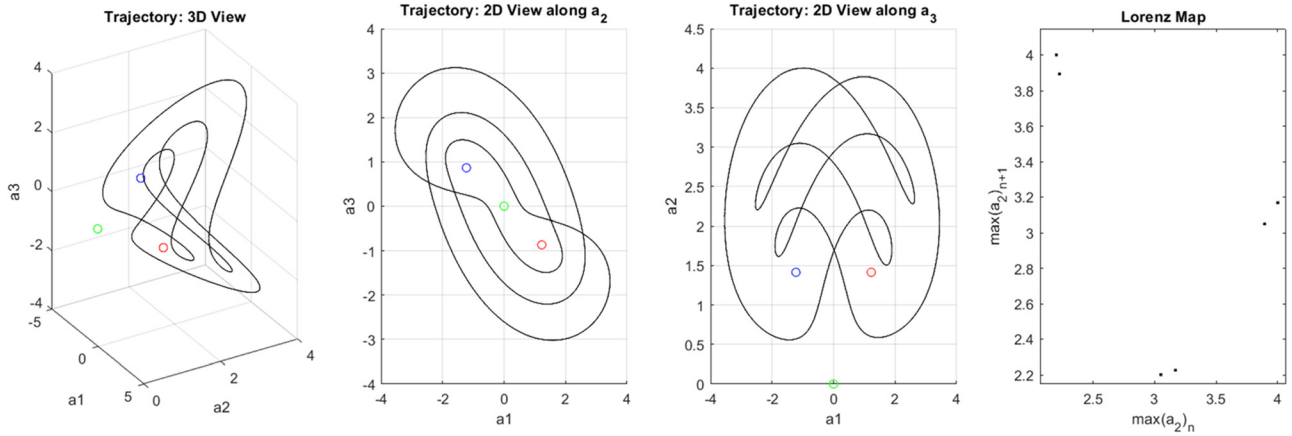

FIG. 5. The trajectory $a_i(t)$ converging to a limit cycle and the Lorenz map (right) found for $\gamma_2 = -0.75$ and $\gamma_3 = -2$.

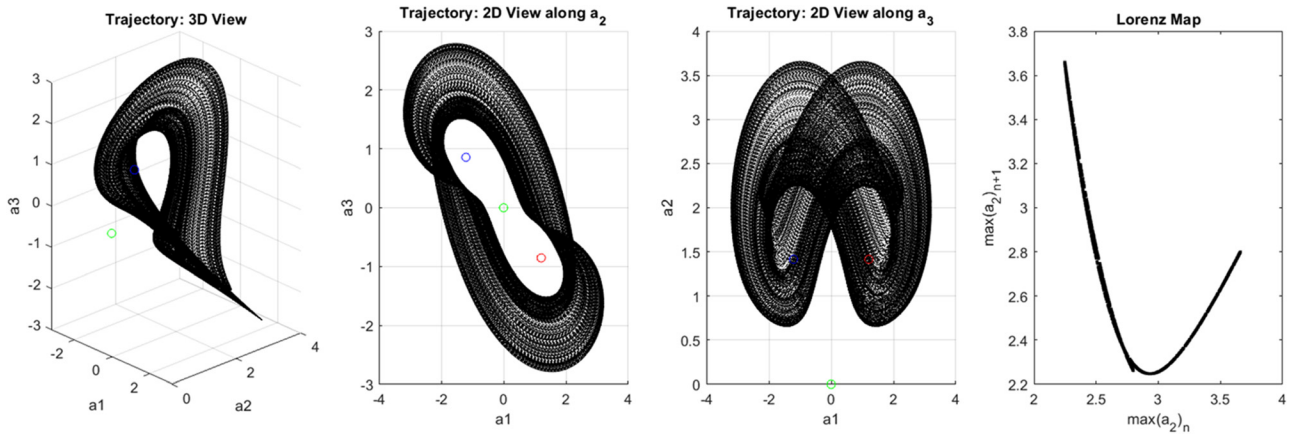

FIG. 6. The trajectory $a_i(t)$ converging to a U-shaped ergodic limit cycle and the Lorenz map (right) found for $\gamma_2 = -0.73$ and $\gamma_3 = -2$.

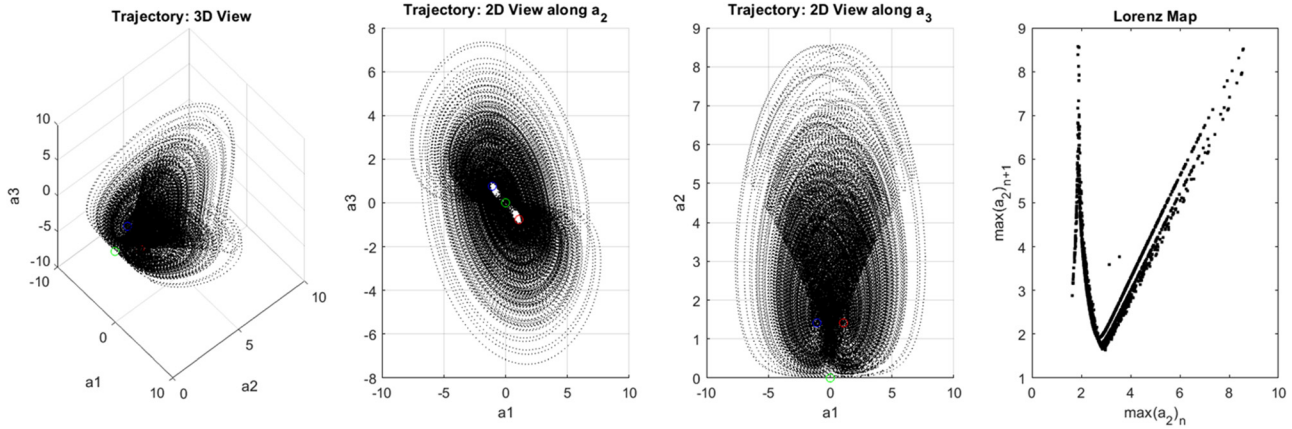

FIG. 7. The trajectory $a_i(t)$ converging to a strange attractor and the N-shape Lorenz map (right) found for $\gamma_2 = -0.58$ and $\gamma_3 = -2$.

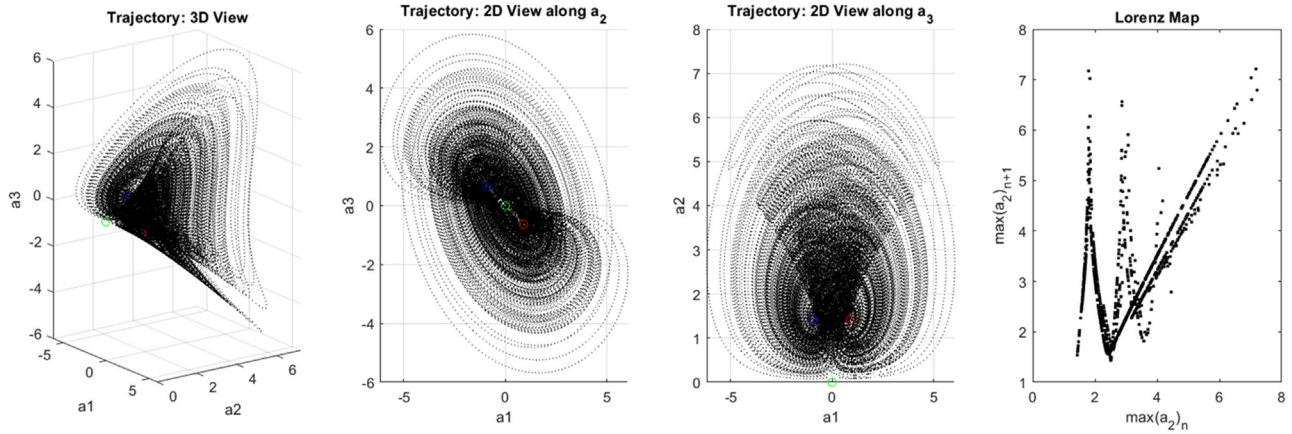

FIG. 8. The trajectory $a_i(t)$ converging to a multi-lobe strange attractor and multi-N-shape curves Lorenz map (right) found for $\gamma_2 = -0.4$ and $\gamma_3 = -2$.

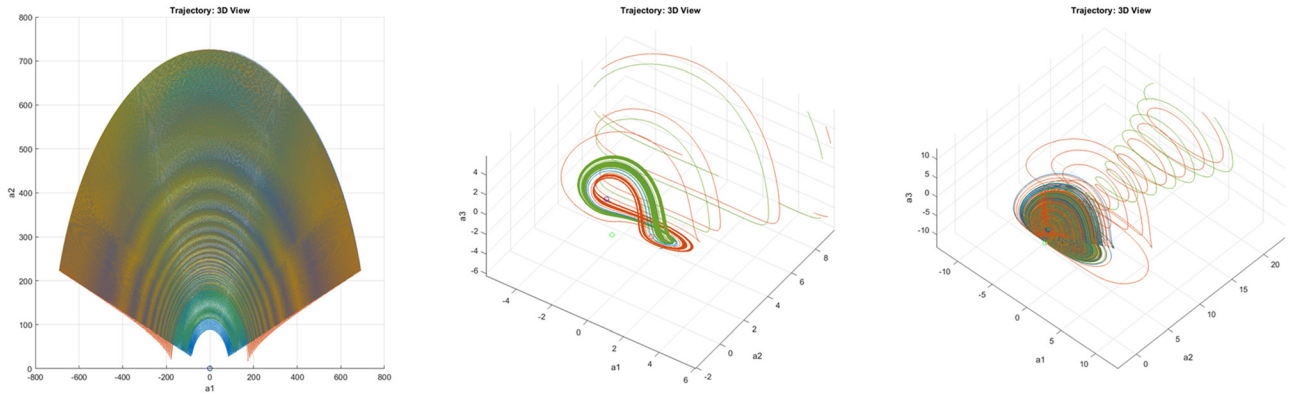

FIG. 9. The trajectories $a_i(t)$ starting from three different initial conditions: (2, 1, −1) (blue), (50, 50, 0) (green), and (100, 1, −100) (red), and all converging the same behavior: exponential growth as shown in Fig. 1, an ergodic limit cycle as shown in Fig. 4, and a strange attractor as shown in Fig. 8.

two consecutive maxima of $a_2(t)$ with respect to each other, in other words, $\max(a_2(t))_{n+1}$ vs $\max(a_2(t))_n$. Likewise, the stationary points are visible on all Figs. 1–9 as colored circles, which the solution trajectory orbits around.

As we see from Fig. 1, the Lorenz map for an unbounded trajectory exhibits a straight line with a positive slope, which shows continuous growth of the function $a_2(t)$. For the case of the various limit cycles shown in Figs. 2–6, the Lorenz map varies from a very small, but still finite region in Fig. 2, to the U-shape curve in Fig. 6. The transition to the strange attractor drastically changes corresponding Lorenz map, which starts to resemble N-like shape (see Fig. 7). We notice that unbound oscillating trajectories and the trajectories converging to both ergodic limit cycles and strange attractors were also found in Ref. 18. For the case of the multi-lobe strange attractor, the Lorenz map becomes the superposition of few N-like curves (see Fig. 8).

In Fig. 9, we demonstrate the convergence of the trajectories $a_i(t)$ starting from three different initial conditions to, correspondingly, an unbounded trajectory, shown in Fig. 1, an ergodic limit cycle, shown in Fig. 4, and a strange attractor, shown in Fig. 8.

Thus, we find that all bounded solutions of Eq. (1) are "attractors," in the sense that they attract all trajectories $a_i(t)$ independently on initial conditions. As a result, the type of trajectory only depends on the magnitudes of the growth rates γ_2 and γ_3 (recall that in normalized units, we have $\gamma_1 = 1$). Therefore, we can map the regions occupied by different types of trajectories on the plane (γ_2, γ_3). To accomplish this goal, we perform parallel simulations of Eq. (1) with different values of γ_2 and γ_3, gradually changing their values. In the domains of γ_2 and γ_3 within (−1, 0) and (−20, −1), we advance the growth rates with the steps −0.1 and −0.25, respectively.

To characterize different attractors, we fit a variety of curves, such as lines and parabolas, to the scatterplot of the Lorenz maps. The decision to what type of attractor the trajectory belongs to is based on the coefficient of determination R^2, which describes the goodness of the fit. Our findings are shown in Fig. 10. It is evident in this finding that the stability of the trajectory follows a non-trivial dependence on γ_2 and γ_3, slipping into and out of regions of stability or chaos. This is visible in the pattern of progression in Figs. 4–8, where $\gamma_3 = -2$ is held constant with changing γ_2, resulting in a progression from a limit cycle to an ergodic limit cycle, back to a limit cycle, before a full

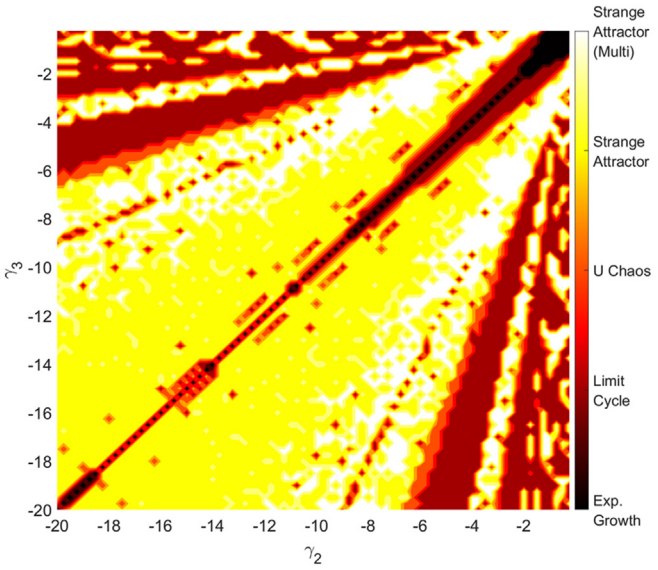

FIG. 10. Regions on the plane (γ_2, γ_3) occupied by different types of trajectories $a_i(t)$ found from the solutions of Eq. (1).

descent into strange attractors. This behavior is visible in the map of the parameter space, with lines of stable limit cycles breaking up the sea of strange attractors (the lack of resolution makes these lines appear as series of points).

At the start of this analysis, we limited ourselves to consider real-valued wave amplitudes $a_i(t)$; however, a cursory analysis of the complex-valued case revealed only unbounded oscillations and little else of interest.

In conclusion, the "real-world" instances of resonant three-wave interactions frequently occur in spectra consisting of many superimposed waves that arrange to form complicated resonance clusters of triads and quartets that interact nonlinearly and turbulently (e.g., see Ref. 13 and the references therein). However, even in the simplest case of one triad, stochastic variation of the wave amplitudes is still possible with the addition of linear growth terms.

This work was supported by the U.S. Department of Energy, Office of Science, Office of Fusion Energy Sciences under Award No. DE-FG02-04ER54739 at UCSD.

AUTHOR DECLARATIONS

Conflict of Interest

The authors have no conflicts to disclose.

Author Contributions

Yevgeniy V Yakusevich: Investigation (equal); Software (equal); Writing – original draft (equal). **Sergei Krasheninnikov:** Supervision (equal); Writing – review and editing (equal).

DATA AVAILABILITY

The data that support the findings of this study are available from the corresponding author upon reasonable request.

REFERENCES

[1]V. E. Zakharov, V. S. L'vov, and G. Falkovich, *Kolmogorov Spectra of Turbulence*, Series in Nonlinear Dynamics (Springer-Verlag, New York, 1992).
[2]D. C. Fritts and M. J. Alexander, "Gravity wave dynamics and effects in the middle atmosphere," Rev. Geophys. **41**, 1–64, https://doi.org/10.1029/2001RG000106 (2003).
[3]C. P. Connaughton, B. T. Nadiga, S. V. Nazarenko, and B. E. Quinn, "Modulational instability of Rossby and drift waves and generation of zonal jets," J. Fluid Mech. **654**, 207–231 (2010).
[4]V. I. Erofeev, *Wave Processes in Solids With Microstructure* (World Scientific, Singapore, 2003).
[5]Y. Kuramoto, "Chemical oscillations," in *Waves and Turbulence* (Springer, New York, 1984).
[6]N. B. Janson, "Nonlinear dynamics of biological systems," Contemp. Phys. **53**, 137–168 (2012).
[7]R. Carretero-Gonzalez, D. J. Frantzeskakis, and P. G. Kevrekidis, "Nonlinear waves in Bose–Einstein condensates: Physical relevance and mathematical techniques," Nonlinearity **21**, R139–R202 (2008).
[8]B. B. Kadomtsev, *Plasma Turbulence* (Academic Press, London, 1965).
[9]R. Z. Sagdeev and A. A. Galeev, *Nonlinear Plasma Theory* (Benjamin, New York, 1969).
[10]V. N. Tsytovich, *Nonlinear Effects in Plasma* (Plenum, New York, 1970).
[11]A. A. Vedenov, A. V. Gordeev, and L. I. Rudakov, "Oscillations and instability of a weakly turbulent plasma," Plasma Phys. **9**, 719–735 (1967).
[12]P. H. Diamond, S.-I. Itoh, K. Itoh, and T. S. Hahm, "Zonal flows in plasma: A review," Plasma Phys. Controlled Fusion **47**, R35–R161 (2005).
[13]E. Kartashova, *Nonlinear Resonance Analysis, Theory, Computation, Application* (Cambridge University Press, 2010).
[14]J. Dominski and A. Diallo, "Transition of a network of nonlinear interactions into a regime of strong nonlinear fluctuations: A paradigm for the edge localized mode onset," Phys. Plasmas **28**, 092306 (2021).
[15]L. Stenflo, "On the equilibrium states of interacting waves," Z. Phys. **243**, 341–345 (1971).
[16]P. Lynch, "On resonant Rossby–Haurwitz triads," Tellus A **61**, 438–445 (2009).
[17]S. A. Galkin and S. I. Krasheninnikov, "On the sink-source effects in two-dimensional plasma turbulence," Phys. Plasmas **8**, 5091–5095 (2001).
[18]S. I. Krasheninnikov and A. R. Knyazev, "Resonance three-wave interactions and strange attractor," Phys. Plasmas **29**, 010702 (2022).
[19]E. N. Lorenz, "Deterministic nonperiodic flow," J. Atmos. Sci. **20**, 130–141 (1963).
[20]O. E. Rössler, "An equation for hyperchaos," Phys. Lett. A **71**, 155–157 (1979).
[21]G. A. Leonov and N. V. Kuznetsov, "On differences and similarities in the analysis of Lorenz, Chen, and Lu systems," Appl. Math. Comput. **256**, 334–343 (2015).
[22]H.-O. Peitgen, H. Jürgens, and D. Saupe, *Chaos and Fractals: New Frontiers of Science* (Springer, 2004).
[23]S. H. Strogatz, *Nonlinear Dynamics and Chaos*, 2nd ed. (CRC Press, 2018).
[24]H. Wilhelmsson, L. Stenflo, and F. Engelmann, "Explosive instabilities in the well-defined phase description," J. Math. Phys. **11**, 1738 (1970).